



7-11-4

## AN EXPERIMENTAL STUDY ON ACTIVE MASS DAMPER

Satoru AIZAWA<sup>1</sup>, Yasuzo FUKAO<sup>1</sup>, Shigeru MINEWAKI<sup>1</sup>,  
Yutaka HAYAMIZU<sup>1</sup>, Hiroshi ABE<sup>2</sup> and Nobuyoshi HANIUDA<sup>3</sup>

<sup>1</sup>Takenaka Technical Research Laboratory, Tokyo, Japan

<sup>2</sup>Office of Advanced Engineering Structure, Takenaka Corporation,  
Tokyo, Japan

<sup>3</sup>Technology Research Center, KAYABA INDUSTRY Co., Ltd. Kanagawa,  
Japan

### SUMMARY

Authors began to study on active structural control aiming to reduce the response of a structure during earthquakes. In this paper, the algorithm of the active mass damper using the optimal control theory and the results of 4-story frame model tests are shown. The optimal control algorithm is formed considering the ability of a mass damper. Against sine wave excitation, the active mass damper was very effective. Against various seismic wave, the mass damper showed a decrease in displacements of 26% to 60% at the maximum value of the response in the uncontrolled case.

### INTRODUCTION

As a concept for designing buildings which are safe against horizontal external forces such as earthquakes and winds, the so-called 'aseismic design method' has, as is well known, been used since for some time and has greatly developed in Japan. In recent years, on the other hand, a practical use of the base isolated construction has progressed which reduces acceleration response during earthquakes by installing elements, which have less horizontal rigidity, at the foundation of a short-period structure and intentionally making the predominant period of the entire frame construction into a long period. Further, damping constructions, in which energy absorbing units are installed into the structure to minimize the response magnification, have been studied for many years and buildings to which this concept applied are also occasionally found. However, the vibration characteristics of these constructions including the damping units against external forces such as earthquakes and winds are constant, and the response quantity is determined by the degree of adaptability to the vibration characteristics of the external force, and thus it does not necessarily follow that all responses to uncertain external force become smaller. Authors began to study ACTIVE MASS DAMPER using optimal control design, as a method of active structural control to undefined force like earthquakes. The outline of these studies is given below.

### ALGORITHM OF ACTIVE MASS DAMPER

The active mass damper system using the optimum control theory which has been developed in the field of mechanical engineering calculates the optimum control force with respect to a system including the active mass unit, and controls

the system from the state quantity of the structure and mass damper unit which change from moment to moment (state feedback control). The active mass damper is a method which uses a mobile mass as a reaction to the control force.

Fig. 1 shows the conceptual diagram of the electrical-hydraulic servo system which has been tested at this time, and Fig. 2 shows the outline of the test apparatus.

Differential Equations of the System In Fig. 1, equations of motion at each mass points are expressed by the following equations:

$$\text{Mobile mass} : M_2(\ddot{x}_2 + \ddot{y}) = U \quad (1)$$

$$\text{Structure} : M_1(\ddot{x}_1 + \ddot{y}) + C_1\dot{x}_1 + K_1x_1 = F - U \quad (2)$$

$$\text{Control force} : U = A(P_1 - P_2) - C_2(\dot{x}_2 - \dot{x}_1) - K_2(x_2 - x_1) \quad (3)$$

where  $M_1, C_1, K_1$ : mass, damping coefficient and stiffness of structure

$M_2$  : Mobile mass       $y$ : Seismic acceleration

$x_1, x_2$  : Displacement of structure and mobile mass

$C_2, K_2$  : Damping coefficient and stiffness of actuator

$A$  : Cylinder area of actuator

$P_1, P_2$  : Cylinder pressure values of actuator

Equations of the State and Output of the System The equation for state of the system is expressed by the following equation using state variable vector  $\{x\}$  and the input  $u$ :

$$\dot{\{X\}} = [A]\{X\} + b u \quad (4)$$

$$\text{where } \{X\} = \{\Delta x_1, \Delta x_2', \Delta \dot{x}_1, \Delta \dot{x}_2'\}^T$$

$$u = i, \text{ i: servo current}$$

$$\Delta x_2' = \Delta(x_2 - x_1)$$

Assuming that output vector  $\{Y\}$  is  $\{Y\} = \{\Delta x_1, \Delta x_2', \Delta \dot{x}_1\}^T$ ,

the output equation can be expressed by  $\{Y\} = [C]\{X\}$  (5)

Control System Theory (design of optimum Regulator) The mechanism which can automatically and quickly return the deviation to the original state is ordinarily constructed by using a feedback and called a 'Regulator'. The method of how to compose the Regulator which shows the best compensating operation under a given evaluation standard is referred to as the problem of the optimum regulator.

In the control system expressed by eqs. (4) and (5), the evaluation function  $J$  is assumed to be as follows:

$$J = \int_0^{\infty} (\{Y\}^T [Q] \{Y\} + ru^2) dt \quad (6)$$

where  $[Q]$  and  $r$  are weights. The above equation indicates that when  $Q$  is made larger, instant responsiveness increases, and  $r$  is increased, control input becomes smaller.  $[Q]$  is obtained by

$$[Q] = \begin{bmatrix} q_1 & 0 \\ 0 & q_2 \\ 0 & q_3 \end{bmatrix} \quad (7)$$

The optimum input  $u^*$  which minimizes the evaluation function  $J$  is expressed by the following equation using the optimum feedback vector  $\{f^*\} = \{f_1, f_2, f_3, f_4\}^T$ :

$$u^* = \{f^*\}^T \{X\} \quad (8)$$

This optimum feedback vector  $\{f^*\}$  is given by:

$$\{f^*\}^T = -r^{-1} \{b\}^T [P] \quad (9)$$

provided that  $[P]$  is an orthodox and unique solution which can satisfy the following Ricatti's equation of matrix:

$$[P][A] + [A]^T [P] - [P]\{b\}r^{-1}\{b\}^T [P] + [Q] = 0 \quad (10)$$

The following optimum closed loop system obtained by substituting eqs. (8) and (9) in eqs. (4) is called the optimum regulator:

$$\{\dot{X}\} = ([A] - \{b\}r^{-1}\{b\}^T [P])\{X\} \quad (11)$$

Finally the control force is

$$\Delta U = D_1 \Delta i - D_2 \Delta \dot{x}'_2 \quad (12)$$

where  $D_1, D_2$  are coefficients determined from the actuator.

#### TEST MODEL

Test Specimen Frame The steel-skeleton four-story frame shown in Fig. 3 was used as a test specimen. Measuring points are shown in the figure. The primary equivalent mass, stiffness and damping coefficient for the regulator designing purpose are shown in Table 1.

Active Mass Damper Fig. 4 shows the active mass damper. The mobile mass can be adjusted to 9 kg and 12 kg. The maximum stroke is 13 cm. For state variables, the relative displacement and velocity of the frame and the mobile mass were used. The weighting of the various output variables and control input of regulators used in the tests is shown in Table 2.

#### TEST RESULTS AND DISCUSSION

Sine Wave Excitation Tests Fig. 5 shows the top floor displacement resonance curves in the uncontrolled case and in the case of using regulators A1 and B1. When the active mass damper is performed, the maximum response magnification was about 1/60 to 1/70, 1/10 and 1/4 at the 1st, 2nd and 3rd resonant frequencies respectively compared with the uncontrolled case. Simultaneously the peak vibration frequency shifts to a slightly lower frequency. Both regulators A1 and B1 show a primary peak frequency of 0.5 Hz or in that proximity and shift toward the lower frequency side by about 30% compared with the results in the uncontrolled case. Fig. 6 shows the maximum response magnification of each story near resonant frequency and the vibration modes at a time in the uncontrolled case and with the regulator A1. The figure indicates the effects of the mass damper up to the 3rd mode. Table 3 shows the damping ratios of the frame obtained from the free vibration waveform at a predominant frequency. It indicates that at the same weighting, damping ratios are nearly equal, and show damping of about 50 times, 35 times and 7 times of the results in the uncontrolled case viewed from order of weighting.

Seismic Wave Excitation Tests Table 4 shows the maximum values of the relative displacement and acceleration of the top-story in various seismic wave excitation tests. Figure in the parentheses indicates the ratio to the uncontrolled cases. It indicates that for regulator B1, the maximum value of relative displacement comes to be 26 to 59% that of the uncontrolled cases and of regulator B7 comes to 45 to 77%, thereby demonstrating the damping effect. Regulator B10 hardly shows any effect. Regulator A1, A7, A10 show similar tendency. Among regulators having the same weighting, that with a mobile mass of 12 kgf (B Series) shows a damping effect of about 10 to 30% greater than the regulator with a mobile mass of 9 kgf (A Series).

Fig. 7 shows the examples of waveforms in the uncontrolled case and with the regulator B1, when Hachinohe wave is inputted. Fig. 8 shows the examples of Fourier spectra of acceleration. The reason why the maximum acceleration value of the weighted regulators has not been reduced compared with the uncontrolled cases is deemed attributable to the comparatively higher vibration components above 3 Hz which are seen in the acceleration Fourier spectra at the top floor in Fig. 8.

Motions of the Mobile Mass Table 5 shows the maximum values of the stroke quantities and control forces of a mobile mass when the sine wave near the primary resonant frequency and Hachinohe wave are input. It indicates that regulators with same weighting are compared, control forces are nearly equal and stroke quantities are inversely proportional to the magnitude of the mobile mass, when the sine wave is input, whereas when Hachinohe wave is input, each regulator shows nearly equal stroke quantities, and the ratio between control forces is nearly equal to that between mobile masses. Control forces in regulators A10 and B10 are about 60% of regulators A1 and B1 in the case of inputting sine waves, but in the case of inputting Hachinohe wave, control forces of A10 and B10 are about 25% of B1. Acceleration Fourier spectra of mobile mass includes peaks of high frequency as well as peaks of less than 2 to 3Hz which are seen in the input. This fact can well explain the shape of the acceleration Fourier spectra at the top floor and results the greater maximum acceleration than that in the uncontrolled case.

## CONCLUSION

Sine wave and seismic wave excitation tests were carried out with respect to active mass damper using the optimum regulator in the modern control theory. According to the results of the tests, the following can be said:

i) Against sine wave excitation, a damping effect was observed up to the vicinity of the 3rd resonant frequency. Against various seismic waves, the active mass damper shows a decrease in displacement of 26 to 59% at the maximum value compared with the results in the uncontrolled cases. The reason why acceleration does not decrease may be attributable to higher frequencies of input wave or to the relative displacement control theory which has been used in this case.

ii) With respect to the seismic wave input, a greater damping effect can be obtained as the mobile mass becomes greater. In the case of a regulator with a smaller instant responsiveness, the damping effect becomes smaller for the non-steady input than for the steady one.

iii) As mentioned above, the active mass damper in which the optimum regulator under the modern control theory is used as a method to reduce vibrations shows great possibilities, and the authors will examine these possibilities.

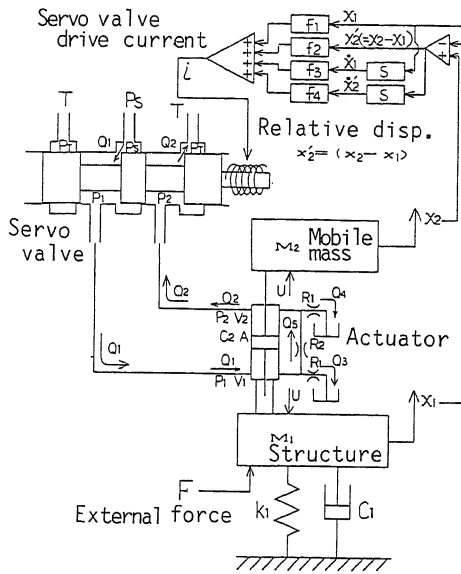


Fig. 1 Conceptual Diagram of the System

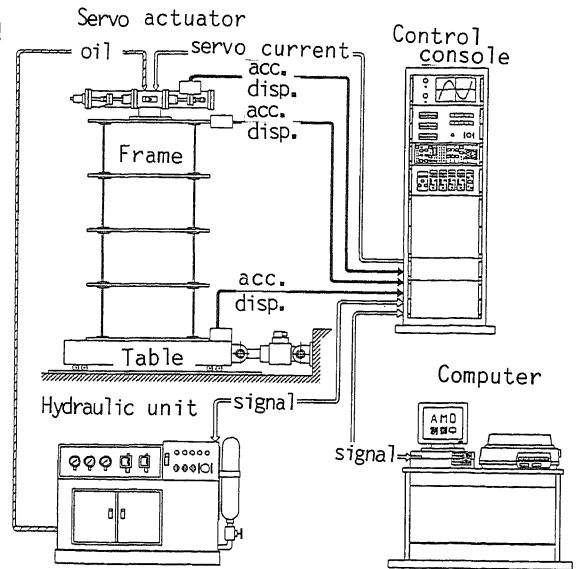


Fig. 2 Outline of Testing Apparatus

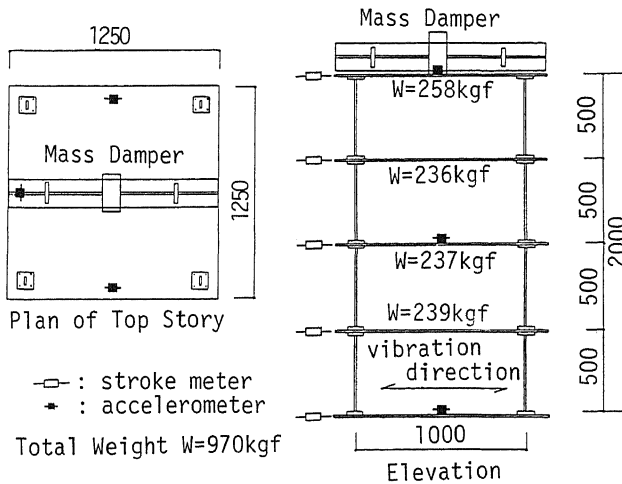


Fig. 3 Test Specimen Frame

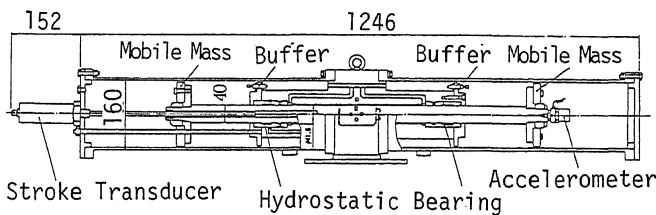


Fig. 4 Actuator and Mobile Mass

Table 1 Values for Designing Regulator

Effective Mass.	$M=0.355 \text{ kgf} \cdot \text{s}^2/\text{cm}$
Effective Stiff.	$K=7.627 \text{ kgf}/\text{cm}$
Effective Damp.	$C=0.011 \text{ kgf} \cdot \text{s}/\text{cm}$

Table 2 Weighting in Evaluation Function

No.	W	$X_1$	$X_2'$	$\dot{X}_1$	u
A 1	9	1	10	6000	1
A 7	9	1	10	500	1
A10	9	1	10	20	1
B 1	12	1	10	6000	1
B 7	12	1	10	500	1
B10	12	1	10	20	1

W : Weight of Mobile Mass (kgf)

$X_1, \dot{X}_1$ : Relative Disp. and Vel. at The Top Story

$X_2'$ : Stroke Quantity of Mobile Mass

u : Control Input

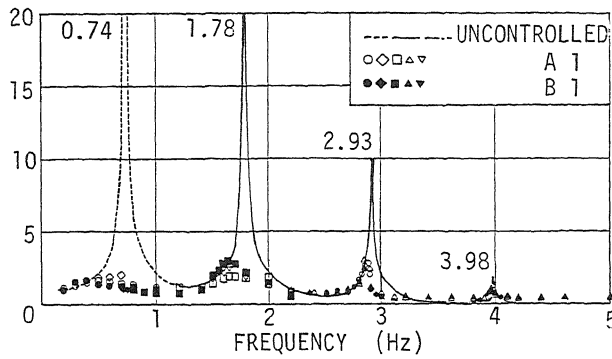


Fig. 5 Amplification Curve of Displacement at Top Floor

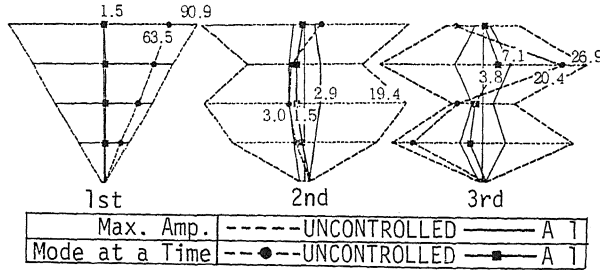


Fig. 6 Maximum Amplification at Each Floor and Vibration Mode at a Time

Table 3 Damping Ratio from Free Vibration

REGULATOR	OFF	A 1	B 1	A 7	B 7	A10	B10
h (%)	0.6	29	30	22	21	3.5	4.3

Table 4 Maximum Response at Top Floor at Seismic Wave Excitation (input:10GAL)

INPUT		UNCONTROLLED		REGULATOR							
		9Kgf	12Kgf	A 1	B 1	A 7	B 7	A10	B10		
EL CENTRO 1940 NS	REL. DISP.	2.1 mm	2.2	1.4 (0.67)	1.3 (0.59)	1.9 (0.90)	1.7 (0.77)	2.4 (1.14)	2.3 (1.05)		
	ACC.	9.8 gal	9.1	10.3 (1.05)	13.6 (1.49)	13.7 (1.40)	12.1 (1.33)	10.6 (1.08)	0.88 (0.97)		
TOKYO 101 1956 NS	REL. DISP.	3.0	3.2	1.7 (0.54)	1.6 (0.50)	2.7 (0.90)	2.2 (0.69)	3.3 (1.10)	3.0 (0.94)		
	ACC.	13.0	12.5	12.7 (0.98)	16.7 (1.34)	15.0 (1.15)	11.8 (0.94)	13.0 (1.00)	11.4 (0.91)		
HACHINOHE 1963 EW	REL. DISP.	6.6	6.4	2.0 (0.30)	1.8 (0.26)	3.3 (0.50)	3.1 (0.45)	6.5 (0.98)	6.1 (0.88)		
	ACC.	16.2	17.4	15.1 (0.93)	22.9 (1.32)	17.3 (1.07)	18.4 (1.06)	17.3 (1.07)	19.5 (1.12)		

Table 5 Maximum Values of Mass-Stroke and Control Force

INPUT	STROKE QUANTITY (CM)						CONTROL FORCE (kgf)					
	A 1	B 1	A 7	B 7	A10	B10	A 1	B 1	A 7	B 7	A10	B10
EX-1	5.8	4.8	3.6	2.6	2.3	1.8	0.76	0.84	0.64	0.67	0.49	0.48
EX-2	12.0	11.6	5.4	5.6	1.4	1.7	6.1	8.7	4.9	5.9	1.5	2.2

EX-1: SINE WAVE, 1.14 GAL. EX-2: HACHINOHE 10 GAL.

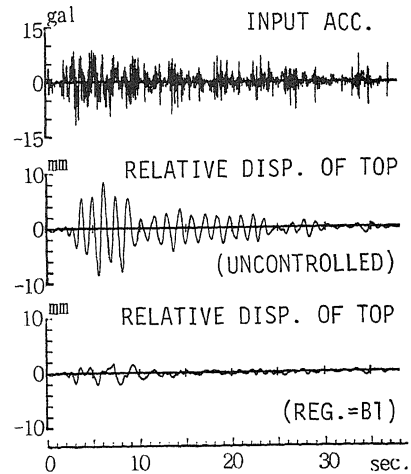


Fig. 7 Effect of Control

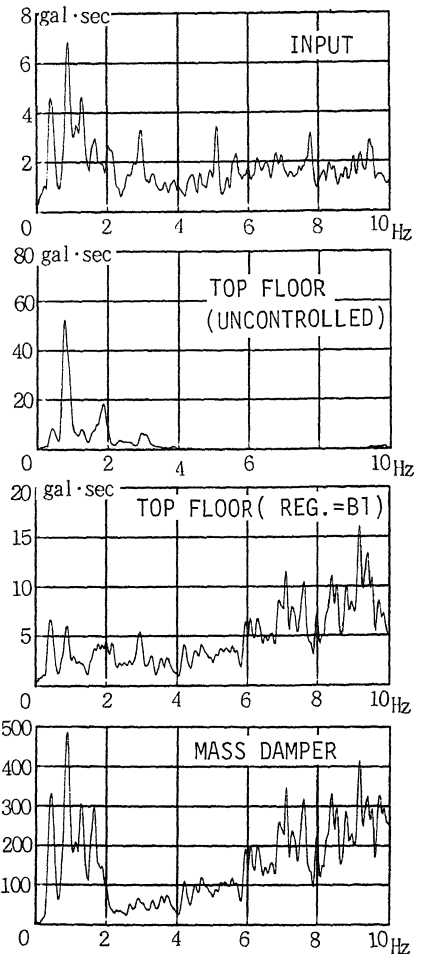


Fig. 8 Acceleration Fourier Spectra (input:HACHINOHE)